Crystal growth, structural, spectral and NLO studies of L-histidine sodium chloride crystals

S. Sudharthini[1], P. Selvarajan [2] & C. Gnana Sambandam[3]

[1]Research Scholar, Reg. No. 12358, Department of Physics and Research Centre, S. T. Hindu College, Nagercoil-629002, Tamilnadu, India.

(Assistant Professor, Francis Xavier Engineering College, Tirunelveli-627003, Tamilnadu, India)

(Affiliated to Manonmaniam Sundaranar University, Abishekapatti-627012, Tirunelveli, Tamilnadu, India)

[2]Department of Physics, Aditanar College of Arts and Science, Tiruchendur-628216, Tamilnadu, India.

[3]Department of Physics, S. T. Hindu College, Nagercoil-629002, Tamilnadu, India.

Abstract

Nonlinear optical (NLO) crystals are useful in generating UV and visible laser light and hence they are called laser crystals and have applications in laser technology, opto-electronics, optical communication and optical computing. NLO crystals can be mainly classified into organic, inorganic and semiorganic NLO materials. In this work, a semiorganic NLO crystal viz., L- histidine sodium chloride (LHSC) has been grown by slow evaporation technique. The grown crystals were transparent and white in color. The solubility study has been carried out in the temperature range 30 ^{o}C-50^{o}C in double distilled water. The lattice parameters of the grown crystals were obtained by single crystal X-ray diffraction technique. The presence of the functional groups in the crystal lattice was confirmed by Fourier Transform Infrared (FTIR) spectral analysis. The UV-visible spectral studies were carried out to find the transmittance and other optical parameters. The presence of elements in the grown crystal was identified by EDAX studies. The TG/DTA studies of the sample were performed to find the thermal stability. Other studies like SHG, LDT and photoluminescence studies for LHSC crystals were also carried out and the obtained results have been discussed.

Key words: Amino acid complex; semiorganic; NLO; single crystal; solution growth; XRD; FTIR; TG/DTA; SHG; LDT; Photoluminescence

1. Introduction

It is well known that nonlinear optical (NLO) crystals have the potential applications in optical information storage, optical logic gates, laser radiation protection, optical communication and optical computing [1,2]. Organic and inorganic NLO crystals have their own limitations. Organic materials may suffer from problems, such as volatility, low thermal stability, mechanical weakness but they have large nonlinear optical characteristics. Inorganic materials have high thermal stability; high hardness but they have low nonlinear optical characteristics. To consider the advantages of both organic and inorganic materials, semiorganic materials are prepared. Semiorganic compounds illustrate the features like dipolar structure composed of an electron donating and electron accepting group, the contribution from the delocalized π electrons belonging to organic ligand results in high nonlinear optic and electro-optic coefficients [3,4]. Efforts have been made on amino acids with organic and inorganic complexes, in order to improve the chemical stability, laser damage threshold, and linear and non-linear optical properties. The importance of amino acid for NLO application lies on the fact that almost all amino acids contain an asymmetric carbon atom and crystallize in non-centrosymmetric space group. Amino acids are organic materials and they can be combined to form semiorganic materials [5, 6]. L-histidine ($C_6H_9N_3O_2$) is an interesting amino acid and it has has a five membered imidazole ring attached to alanine [7,8]. In this work, L-histidine is mixed with sodium chloride to form L-histidine sodium chloride crystal. The objective of the work is to grow the single crystals of L-histidine sodium chloride (LHSC) and to characterize the grown crystals by various studies such as structural studies, optical studies, mechanical studies, thermal studies, electrical studies, spectral and NLO studies.

2. Synthesis and growth of crystals

L-histidine sodium chloride (LHSC) salt was synthesized from stoichiometric incorporation of AR grade of L-histidine and sodium chloride in the molar ratio of 1:1. The reactants were dissolved in double distilled water and mixed thoroughly using a magnetic stirrer at room temperature. On evaporating the solvent by heating at 50^{o} C, the synthesized salt was extracted. The purity of the synthesized salt was further improved by successive re-crystallization process. Using the water as the

solvent and the synthesized salt of LHSC, the saturated solution was prepared. The solution was stirred well using the magnetic stirrer for about 4 hours and it was filtered using the good quality Whatman filter papers. The filtered solution was taken in the growth vessel covered with a perforated paper. The growth vessel was kept in a dust-free atmosphere. It took about 35 days to harvest the transparent and colourless crystals of LHSC and the harvested crystal is shown in the figure 1.

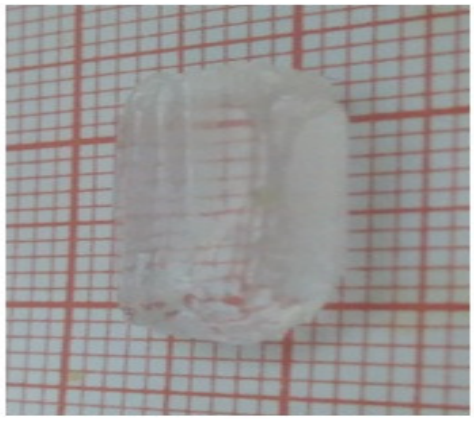

Fig.1: The grown crystal of LSHC

3.Results and discussions

3.1 Solubility studies

The solubility study of the sample was carried out by gravimetric method [9]. The grown crystal was powdered and it was added step by step to 50 ml of water taken in a beaker kept on the hot-plate of magnetic stirrer and stirring was continued till a small precipitate was formed. This gave confirmation of saturated condition of the solution. Then, 25 ml of the solution was pipetted out in a petri dish and it was warmed up till the solvent was evaporated out. By measuring the amount of salt present in the petri dish, the solubility of LHSC in water was determined [10]. The experiment was repeated at different temperatures. The solubility curve of LHSC crystal is shown in the figure 2. From the graph it is observed that the solubility of LHSC sample in water increases linearly with temperature and hence the sample has the positive temperature coefficient of solubility.

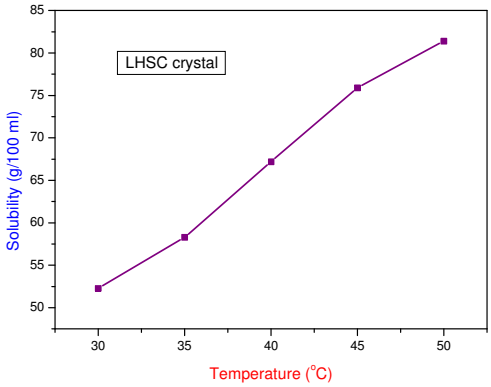

Fig.2: Variation of solubility with temperature for LHSC crystal

3.2 Structural studies

It is known that a crystal can diffract X-rays and this is due to the wavelength of X-rays is almost equal to the interplanar distance of the crystal. The condition of X-ray diffraction (XRD) is the Bragg's law and powder X-ray diffractometer and single crystal X-ray diffractometer are based on the Bragg's law [11]. Since the grown sample in this work is a single crystal, single crystal X-ray diffraction analysis was carried out using a Bruker AXS diffractometer with MoK_α (λ =0.7170 Å) radiation to determine the lattice constants. A small piece of crystal is enough to solve the crystal structure. The obtained lattice parameters of LHSC crystal are a = 7.461(4) Å, b = 6.942(3) Å, c = 11.525(3) Å, α = 90º, β = 90º, γ = 90º. From the result, it is confirmed that LHSC crystal crystallizes in orthorhombic structure.

3.3 FTIR studies

Fourier Transform Infrared (FTIR) technique is an excellent technique for finding the functional and chemical groups of the samples and this method is used to identify the internal structure of the molecule and nature of the chemical bonds of the compounds. In this method, infrared radiation is used and when the frequency of the incident radiation coincides with the vibrational frequency of the molecules, absorption of energy takes place. When the molecule returns from the excited state from ground state the absorbed energy is released resulting in distinct peaks in the IR spectrum [12]. The FTIR spectrum of the grown LHSC crystal was recorded using a

SHIMADZU FTIR spectrometer by the KBr pellet technique in the range 4000 – 400 cm^{-1} and the recorded spectrum is presented in the figure 3. The absorption peak at 3411 cm^{-1} is due to OH stretching and the peak at 3107 cm^{-1} is corresponding to NH_3^+ stretching mode. The CH aliphatic stretching vibration is observed at 2614 cm^{-1} and the absorption peat at 1637 cm^{-1} indicates the NH_3^+ bending mode. OH deformation mode is observed due to the presence of the absorption frequency at 1606 cm^{-1}. The vibrational frequency at 1497 cm^{-1} is due to CN stretching mode. The absorption peaks/bands below 1600 cm^{-1} are corresponding to deformation and bending modes of various functional groups and the FTIR assignments to the absorption frequencies are provided in the table 1. The spectral assignments to the peaks of FTIR spectrum of LHSC crystal are given in accordance with the data reported in the literature [13, 14].

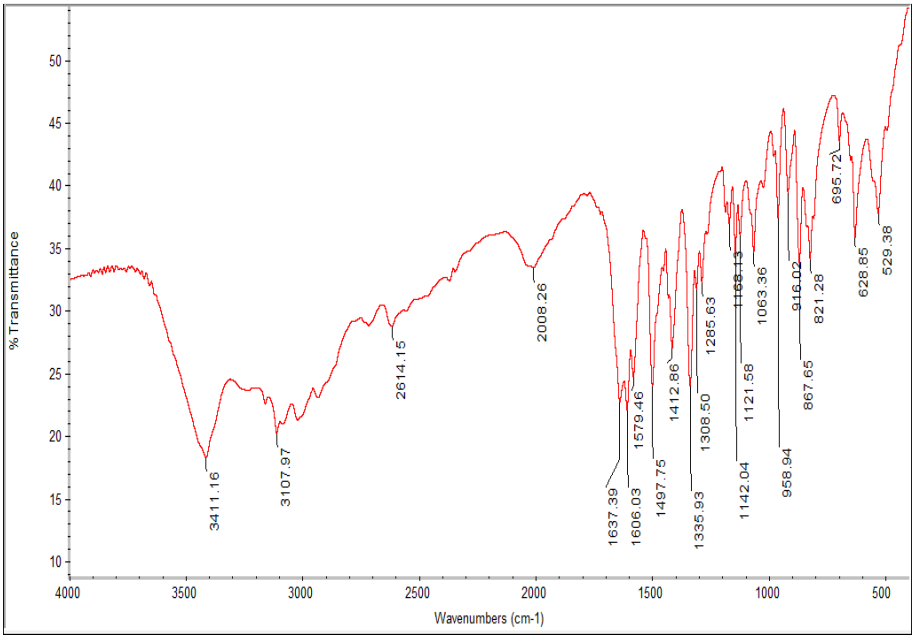

Fig. 3: FTIR spectrum of LHSC crystal

Table 1: The FTIR spectral assignments to LHSC crystal

Wave number $(cm)^{-1}$	Assignments
3411	OH stretching
3107	NH_3^+ stretching
2614	CH stretching
2008	CH_2 stretching
1637	NH_3^+ bending
1606	OH deformation
1579	COO^- stretching
1497	C-N stretching
1412	CH_2 deformation
1335	C-H in plane bending
1308	C-H plane bending
1285	N-H bending
1142	C-H out of plane bending
1121	C-N deformation
1100	Ring deformation
1063	C=O deformation
958	CO stretching
867	C-C deformation
821	CH out of plane bending
695	COO^- scissoring
628	COO^- rocking
529	NH_3^+ rocking

3.4 UV–visible spectral analysis

UV-visible spectroscopy is an important branch of spectroscopy which uses UV, visible and near infrared (NIR) radiations as the incident radiations on the samples and the intensity of transmitted radiation is measured using a detector. The UV-visible transmittance spectrum of LHSC crystal was measured using a Varian Cary 5E UV-Vis-NIR spectrophotometer in the range 190-1100 nm covering the near, visible, near infrared region to find the transmission range to know the suitability of the sample for optical applications. The UV-visible-NIR transmittance and absorbance spectra of LHSC crystal are shown in the figures 4 and 5 respectively. It is observed that the sample shows the UV lower cut-off wavelength at 248 nm and there is a small peak at 298 nm is due to the $\pi - \pi^*$ electron transition. In the visible and NIR regions, there is no appreciable absorption and hence this sample is suitable for production of visible laser light when infrared laser is incident on the sample. The absorption coefficient (α) of the grown crystal was determined from optical transmittance values using the relation $\alpha = (1/t) \ln (1/T)$ where T and t are the transmittance and thickness of the specimen respectively. The absorption coefficient values are used to determine optical energy gap. The band gap energy is an energy range in a solid where no electron states can exist. The band gap energy generally refers to the energy difference (in eV) between the top of the valence band and the bottom of the conduction band of the sample. The relation between the absorption coefficient (α) and the photon energy ($h\nu$) is $(\alpha h\nu)^n = A (h\nu - E_g)$ where E_g is optical band gap of the crystal and A is a constant and this relation is called as the Tauc's relation [15]. Using this relation, a plot is drawn and it is shown in the figure 6. Tauc's plot is a convenient way of displaying the optical absorption/transmittance spectrum of a material and it shows the optical energy on the abscissa and the quantity $(\alpha h\nu)^n$ on the ordinate. The value of the exponent 'n' denotes the nature of the transition, for example, n= ½ for indirect transition and n=2 for direct transition. The obtained optical band gap value from the Tauc's plot for LHSC crystal is 4.97 eV. Using the values of absorption coefficient (α), reflectance values of the sample was determined using the following relation

$$R = 1 \pm (1-\exp(-\alpha t) + \exp(\alpha t))^{1/2} / (1+\exp(-\alpha t))$$

where t is the thickness of the sample [16]. The variation of reflectance with wavelength for LHSC crystal is depicted in the figure 7. It is seen that there is a sudden decrease at the UV cut-off wavelength and it is low and constant in the visible

region. Since transmittance is high and reflectance is low in the visible region, LHSC crystal could be used for the fabrication of electro-optic and optoelectronic devices.

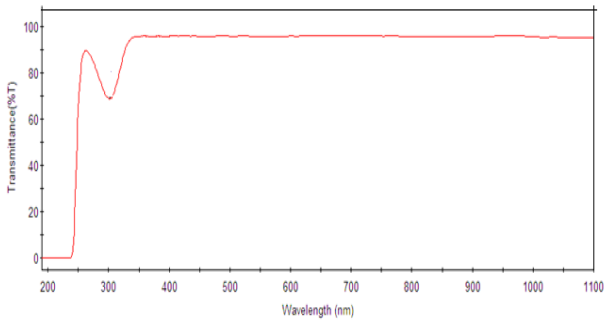

Fig. 4.UV–visible transmittance spectrum of LHSC crystal

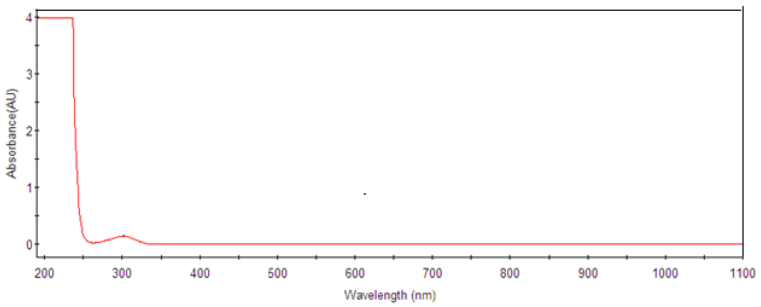

Fig. 5. UV–visible absorbance spectrum of LHSC crystal

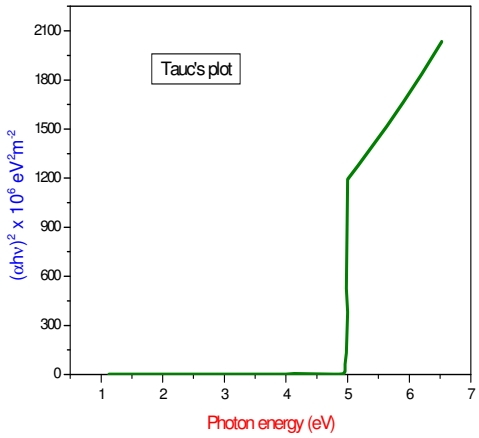

Fig. 6. Tauc's plot for LHSC crystal

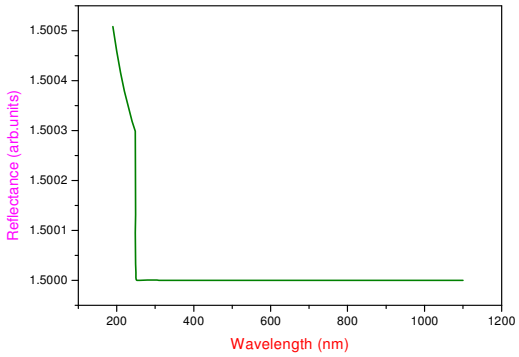

Fig. 7. Variation of reflectance with wavelength for LHSC crystal

3.5 TG/DTA-thermal characterization

The study of thermal stability, endothermic and exothermic transitions, melting point/decomposition point of the sample can be analyzed using the TG/DTA thermal curves. The TG/DTA thermal traces for LHSC crystal are shown in the figure 8 and these curves were recorded using a STD Q600 V8.3 Build 101 thermal analyzer in nitrogen atmosphere for the temperature range 40 ^{o}C -400 ^{o}C at a heating rate of 10 ^{o}C min^{-1}. The figure shows that the sample is thermally stable upto 295 ºC and the weight loss of the sample starts above this temperature. About 7% of weight loss is noticed in the temperature range 300-310 ^{o}C and 13% of weight loss is observed in the temperature range 310-400 ^{o}C. In the DTA thermal curve, there is an endothermic peak at 295 ^{o}C which corresponds to the decomposition point of the sample.

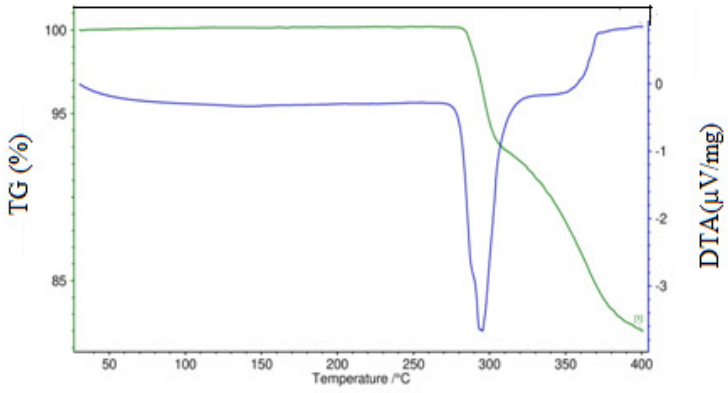

Fig.8: TG/DTA thermal curves for the grown LHSC crystal

3.6 EDAX studies

Energy dispersive X-ray spectroscopy (EDAX) was used to identify the elements present in the grown LHSC crystal. The EDAX spectrum was recorded using Jeol 6390LV model scanning electron microscope and it is shown in the figure 9. From the result, it is confirmed that the elements such as carbon, oxygen, chlorine, sodium and nitrogen are present in the sample. Since hydrogen cannot be identified using the EDAX method, it is not indicated in the spectrum. The weight percentage and atomic percentage of the elements in the grown crystal of LHSC are given in the table 2.

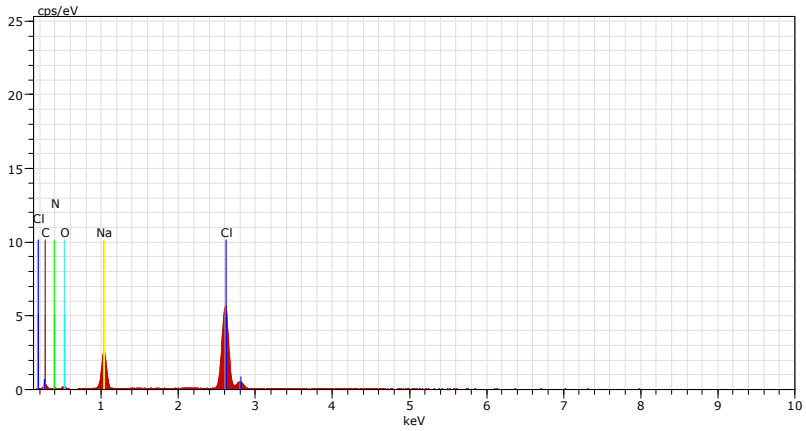

Fig.9: EDAX spectrum of LHSC crystal

Table 2: Weight percentage and atomic percentage of elements present in LHSC crystal

Element	Atomic number	Series	Weight (%)	Atomic %
Cl	17	K-series	34.78	16.74
C	6	K-series	30.75	45.51
O	8	K-series	17.83	19.92
N	7	K-series	8.46	10.73
Na	11	K-series	6.80	5.09

3.7 Measurement photoluminescence

Photoluminescence (PL) is a process whereby the matter generates non-thermal type of optical radiation usually in the visible range, but can also be in other spectral regions such as UV and IR. The spectral energy distribution and time dependence of the emission are related to electronic transition probabilities within the sample, and can be used to provide qualitative and, sometimes, quantitative information about chemical composition, structure, impurities, kinetic processes and energy transfer. Using the photoluminescence experimental set-up and the excitation wavelength of 220 nm., the photoluminescence emission spectrum of LHSC crystal was recorded and it is shown in the figure 10. There are mainly two emission peaks at 487 nm and 740 nm. The high intense peak at 487 nm is corresponding to the emission of bluish light and the peak at 740 nm is due to emission of near infrared radiation.

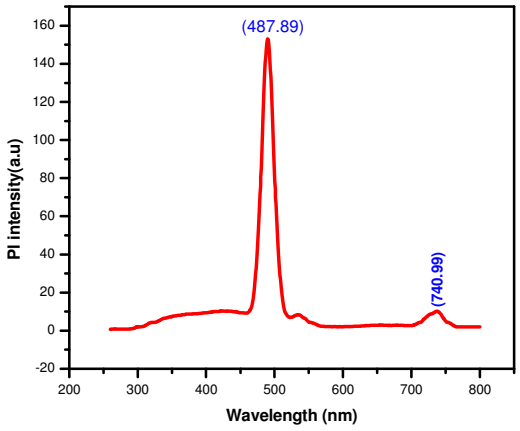

Fig.10: Photoluminescence spectrum of LHSC crystal

3.8 NLO studies

Nonlinear optical (NLO) phenomena can classified into second order NLO, third order NLO and higher order NLO phenomena. Second harmonic generation (SHG) is one of the second order NLO phenomena and in this phenomenon, the frequency of incident laser radiation is converted into double the frequency [17]. SHG measurement was carried out using the experimental set-up of Kurtz-Perry powder method. The grown crystal of LHSC was powdered into particles of size of about 250-300 μm and it was subjected to laser radiation from a Q-switched Nd:YAG laser of wavelength of 1064 nm. The emission of green radiation from the sample give an indication of SHG and the energy of the emitted

radiation was measured by using the power meter. The values in connection with SHG measurement are provided in the table 3.

Table 3: Output energy and relative SHG efficiency for LHSC crystal

Crystal name	Output energy (milli joule/pulse)	Input energy (joule/pulse)	Relative SHG efficiency with respect to KDP
LHSC crystal	13.65	0.71	1.54
KDP crystal	8.81	0.71	1

3.9 Measurement of LDT

Laser damage threshold (LDT) is an important material parameter, the knowledge of which is essential for using the crystal as an NLO element in various applications involving large laser input power like frequency doubling, optical parametric processes, etc. In fact, laser induced damage in optical materials remains the limiting factor in the development of high power laser systems and optoelectronic devices. Using a Q-switched Nd: YAG laser (Continuum USA, Model: Surelite-III) of wavelength 1064 nm and pulse width 10 ns, the value of LDT of LHSC crystal was measured. The energy of the laser pulses was controlled by an attenuator and delivered to the test sample located near the focus of a plano-convex lens. The occurrence of single pulse damage was observed by monitoring the fall of transmitted intensity as detected by a fast PIN type Si photodiode and traced in a digital storage oscilloscope. The LDT value was determined using the formula $P = E/\pi\tau r^2$ where E is the input energy in mJ, τ is the pulse width and r is radius of the spot[18]. The calculated value of LDT for LHSC crystal is 2.47 GW/cm^2 and as this value is high, the title crystal could be used in high power laser applications [19].

4. Conclusions

L-histidine sodium chloride (LHSC) crystals were grown by slow evaporation method and it has the positive temperature coefficient to solubility. XRD studies reveal that LHSC crystal crystallizes in orthorhombic structure. Functional groups have been identified by FTIR method. LHSC crystal has wide transparency in the

visible region and it has the optical band gap of 4.97 eV. The decomposition point of LHSC crystal is 295 ^{o}C. The relative SHG efficiency of LHSC crystal is found to be 1.54 times that of KDP. The LDT value of the sample is calculated to be 2.47 GW/cm^2. The EDAX study helps to find the weight percentage of the elements present in the grown crystal of LHSC. The highest intensity of photoluminescence from the sample is observed at 487 nm.

References

1. V.K Dixit, S. Vanishri, H.L Bhat, E. de Matos Gomes, M. Belsley, C. Santinha, G. Arunmozhi, V. Venkataramanan, F. Proena, A. Criado, J. Crystal Growth 253 (2003) 460-466.
2. P.Selvarajan, J.Glorium Arulraj, S.Perumal, J. Crystal Growth 311 (2009) 3835–3840.
3. P.N. Prasad, D. Williams, Introduction to Nonlinear Optical Effects in Organic Molecules and Polymers, Wiley, New York, 1991.
4. D.S. Chemla, J. Jyss, Nonlinear Optical Properties of Organic Molecules and Crystals, Academic Press, NewYork, 1987.
5. H.O. Mercy, L.F. Warren, M.S. Webb, C.A. Ebbers, S.P. Velsko, G.C. Kennedy and G.C.Catella, Appl. Opt. 31 (1992) 5051.
6. G. Anandha Babu and P. Ramasamy, Materials Chemistry and Physics 113 (2009) 727.
7. S. Dhanuskodi and P.A.A.Mary, J. Crystal Growth, 253 (2003) 424.
8. H.A.Petrosyan,H.A.Karapetyan,A.M.Petrosyan, J.Mol.Struct.,794(2006) 160–167.
9. R. Jothi Mani, P.Selvarajan, H. Alex Devadoss, D. Shanthi, Optik 126 (2015) 213–218.
10. D. Jayalakshmi, R. Sankar, R. Jayavel, J. Kumar, J. Crystal Growth 276 (2005) 243-246.
11. H.P.Klug, L.E.Alexander, X-ray diffraction procedure for polycrystalline and Amorphous materials, 2nd Edn., John Wiley and Sons, New York (1954).
12. C.N.R.Rao, Ultraviolet and Visible Spectroscopy, Butterworths, London (1961).
13. K. Nakamoto, Infrared and Raman Spectra of Inorganic and Coordination Compounds, John Wiley, 5th Ed., London (1997).

14. Reena Ittyachan, P. Sagayaraj, J. Crystal Growth 249 (2003) 553–556
15. J. Tauc, Amorphous and Liquid Semiconductors, Plenum Press, New York (1974).
16. S. Suresh and D. Arivuoli, Lat. Am. J. Phys. Educ. 5 (2011)721-725.
17. M. Narayan Bhat and S. M. Dharmaprakash, J. Crystal Growth, 236, (2002)376–380.
18. Amirdha Sher Gill, S. Kalainathan, J.Phy. Chem. Solids 72 (2011) 1002-1007.
19. K. Rajesh, A. Mani, K. Anandan, P. Praveen Kumar, J Mater. Sci: Mater. Electron.28(2017)11446–11454